Journal of Mathematical Biology (2022) 84:40
https://doi.org/10.1007/s00285-022-01740-4

Mathematical Biology

Spiracular fluttering decouples oxygen uptake and water loss: a stochastic PDE model of respiratory water loss in insects

Sean D. Lawley[1] · H. Frederik Nijhout[2] · Michael C. Reed[3]

Received: 18 June 2021 / Revised: 27 January 2022 / Accepted: 27 March 2022

Abstract
In insect respiration, oxygen from the air diffuses through a branching system of air-filled tubes to the cells of the body and carbon dioxide produced in cellular respiration diffuses out. The tracheal system has a very large surface area, so water loss is a potential threat and the question of how insects regulate oxygen uptake and water loss has been an important issue in insect physiology for the past century. The tracheal system starts at spiracles on the surface of the body that insects can open and close, and three phases are observed experimentally, open or closed for relatively long periods of time and opening and closing rapidly, which is called fluttering. In previous work we have shown that during this flutter phase, no matter how small the percentage of time that the spiracles are open, the insect can absorb almost as much oxygen as if the spiracle were always open, if the insect flutters fast enough. This left open the question of water loss during the flutter phase, which is the question addressed in this paper. We formulate a stochastic diffusion-convection model for the concentration of water vapor in the tracheae. Mathematical analysis of the model yields an explicit formula for water loss as a function of six non-dimensional parameters and we use experimental

The authors gratefully acknowledge research support from the National Science Foundation, DMS-1944574 (SDL), DMS-1814832 (SDL), and IOS-1557341 (HFN, MCR), and the National Institutes of Health, RO1 MH1 06563 (MCR, HFN).

✉ Sean D. Lawley
lawley@math.utah.edu

H. Frederik Nijhout
hfn@duke.edu

Michael C. Reed
reed@math.duke.edu

[1] Department of Mathematics, University of Utah, Salt Lake City, UT 84112, USA

[2] Department of Biology, Duke University, 130 Science Dr, Durham, NC 27708, USA

[3] Department of Mathematics, Duke University, 120 Science Drive, Durham, NC 27708, USA

Published online: 24 April 2022

data from various insects to show that, for parameters in the physiological ranges, water loss during the flutter phase is approximately proportional to the percentage of time open. This means that the insect can solve the oxygen uptake versus water loss problem by choosing to have their spiracles open a small percentage of time during the flutter phase and fluttering rapidly.

Keywords Stochastic switching · Stochastic hybrid system · Random PDE · Piecewise deterministic Markov process · Randomly switching boundary

Mathematics Subject Classification 92C30 · 60J60 · 60H15 · 35R60

1 Introduction

Insects have an efficient mechanism of respiration in which atmospheric air is taken directly to every cell in the body via a progressively more finely branching system of air-filled tubes called the tracheae. Tracheae open to the outside air via a set of openings called spiracles (Wigglesworth 1965). Typically, there is one pair of spiracles per segment, although this arrangement varies considerably among different taxa of insects. Topologically, the tracheal system is an invagination of the body wall, and accordingly, it is lined with a non-living cuticle that is homologous to the exoskeleton. The tracheal system is the principal route for oxygen uptake and for the removal of carbon dioxide produced by metabolism. Because of its large surface area, the tracheal system is also potentially a major avenue of water loss.

Insects have a muscular system by which they can close the spiracles. Closing the spiracles greatly reduces water loss. For instance, when insects are forced to keep their spiracles open, by exposing them to 5% carbon dioxide, their rate of water loss increases two- to ten-fold; the blood-sucking bug Rhodnius prolixus, an otherwise drought resistant species that can live for weeks without access to water, dies from desiccation within 3 days when its spiracles are forced to remain open (Wigglesworth 1965; Wigglesworth and Gillett 1936). Many insects, particularly those that live in dry environments or have little access to water, keep their spiracles closed much of the time, but also exhibit a pattern of discontinuous respiration in which the spiracles alternately open and close for brief periods of time, a phenomenon called fluttering (Wigglesworth 1931; Schneidermann 1956; Contreras et al. 2014). There are also brief periods of time during which the spiracles remain open. These open phases are associated with the rapid release of carbon dioxide, whereas the fluttering phase is associated with oxygen uptake (Buck et al. 1953; Schneiderman 1960; Lighton 1996a; Marias et al. 2005; Matthews and Terblanche 2015). The open phases allow for gas exchange, but also allow water loss, and this presents a dilemma. Ideally, insects need a respiratory system that simultaneously allows for efficient oxygen uptake and minimizes water loss.

We previously studied how the rate of oxygen uptake during the flutter phase depends on the rate of fluttering. Using a mathematical model of oxygen diffusion in the insect tracheal system, we derived a formula for oxygen uptake during the flutter phase that shows how oxygen uptake depends on the length of the tracheal system,

the percentage of time open during the flutter phase, and the flutter rate (Lawley et al. 2020). Our results showed that an insect can have its spiracles closed a high percentage of time during the flutter phase and yet receive almost as much oxygen as if the spiracles were always open, provided that the spiracles open and close rapidly. Thus, insects can regulate their rate of oxygen uptake by varying the rate of fluttering while keeping the spiracles closed a large fraction of the time during the flutter phase.

However, those results left open the question of whether water loss is also increased by rapid fluttering or whether water loss remains proportional to the percentage of time open during the flutter phase. This is the question addressed in this paper. We develop and analyze a stochastic mathematical model to show that water loss in the flutter phase is approximately proportional to the percentage of time the spiracles are open. Thus, insects can achieve both high oxygen intake and low water loss by keeping the spiracles closed most of the time and fluttering rapidly.

The rest of the paper is organized as follows. In Sect. 2, we formulate the mathematical model, which is a one-dimensional diffusion-convection equation with a boundary condition that stochastically switches between two discrete states. The diffusion-convection equation models the water vapor concentration in a tracheal tube, and the switching boundary condition models the opening and closing spiracle. In Sect. 3, we analyze the probability distribution of the solution to this random partial differential equation (PDE) model at large time. In particular, we find the support of this distribution and find an explicit formula for this distribution in a certain physiologically relevant parameter limit. In Sect. 4, we find and analyze the mean of the random PDE by solving an associated deterministic diffusion-convection-reaction boundary value problem. This analysis yields an explicit formula for the average water loss, which we then analyze in several parameter limits. In Sect. 5, we estimate parameter ranges from experimental data on various insects and investigate the physiological implications of the model. In particular, we show that during the flutter phase, water loss is approximately proportional to the percentage of time the spiracles are open. We conclude by discussing our results in the context of prior work.

2 Model formulation

2.1 Dimensional model

Following Lawley et al. (2020), we consider a single spiracle opening to a trachea that branches and ends in a set of tracheoles. We assume that the tracheae branch in such a way that the cross-sectional area remains constant, and this assumption is supported by studies of several types of insects (see Locke (1958) for *Rhodnius*, Krogh (1920) for *Cossus* larva, Thorpe and Crisp (1947) for *Aphelocheirus*, and Weis-Fogh (1964) for *Aeshna* and *Schistocerca gregaria*). Since tracheael tubes are thin, we treat each tube in the tracheal network as one-dimensional. Furthermore, since the cross-sectional area of the tracheae is constant along the tracheal network, we ignore the branching structure (Bressloff and Lawley 2016). In particular, we consider an interval of length $L > 0$, where L is the total length of the tracheal tubes that connect the spiracle to a tracheole.

In our model, the tracheoles are at $x = 0$, the spiracle is at $x = L$, and $\overline{w}(x,t)$ denotes the water vapor concentration in the trachea at position $x \in [0, L]$ at time $t \geq 0$. We assume that $\overline{w}(x,t)$ satisfies the diffusion-convection (advection) equation,

$$\frac{\partial}{\partial t}\overline{w} = D_w \frac{\partial^2}{\partial x^2}\overline{w} - v\frac{\partial}{\partial x}\overline{w} + k(I_w - \overline{w}), \quad x \in (0, L),\ t > 0, \tag{1}$$

where $D_w = 0.282\,\mathrm{cm}^2/\mathrm{s}$ is the water vapor diffusivity (Cussler 2009). The second term in the righthand side of (1) models bulk flow of air into the trachea with velocity $v \leq 0$. The final term in (1) models transfer of water into the trachea through the walls of the trachea. The parameter $k > 0$ is the water transfer rate and $I_w > 0$ is the equilibrium water concentration in the trachea if the spiracle is always closed.

We impose a no flux boundary condition at the tracheoles,

$$-D_w \frac{\partial}{\partial x}\overline{w}(0,t) + v\overline{w}(0,t) = 0,$$

and switching boundary conditions at the spiracle

$$-D_w \frac{\partial}{\partial x}\overline{w}(L,t) + v\overline{w}(L,t) = -b(A_w - \overline{w}(L,t)), \text{ when spiracle open,} \tag{2}$$

$$-D_w \frac{\partial}{\partial x}\overline{w}(L,t) + v\overline{w}(L,t) = 0, \text{ when spiracle closed.} \tag{3}$$

Naturally, (3) imposes a no flux condition when the spiracle is closed. When the spiracle is open, (2) guarantees that the flux out of the spiracle is proportional to the difference between the water vapor concentration at $x = L$ and the ambient water vapor concentration, $A_w > 0$. The constant of proportionality is $b = 4D_w/(\pi a)$ (Bezrukov et al. 2000), where $a > 0$ is the radius of the spiracle. In the case that the tube is long and thin ($a/L \ll 1$), the boundary condition (2) becomes the Dirichlet condition, $\overline{w}(L,t) = A_w$ (one can see this from the dimensionless model in Sect. 2.2 below).

The open and closed durations are known to fluctuate during the flutter phase (Schneiderman 1960; Heinrich et al. 2013), and we take them to be exponentially distributed with a mean that is estimated from experimental data. This means that the boundary condition at $x = L$ switches between (2) and (3) according to a two-state Markov process,

$$\text{open} \rightleftharpoons \text{closed},$$

where $\overline{\alpha}_0 > 0$ is the closing rate and $\overline{\alpha}_1 > 0$ is the opening rate. Also, it is sometimes convenient to work with the percentage of time in the open state and the overall opening/closing rate,

$$p_0 := \frac{\overline{\alpha}_1}{\overline{\alpha}_0 + \overline{\alpha}_1}, \quad r := \overline{\alpha}_0 + \overline{\alpha}_1.$$

A simplified version of this model appeared in our previous work (Lawley et al. 2020) with $v = 0$ and $b = \infty$.

2.2 Dimensionless model

If we rescale space and time, $x \to \frac{1}{L}x$ and $t \to \frac{D_w}{L^2}t$, and define a new dimensionless water concentration $w := \overline{w}/I_w$, then the model reduces to the following dimensionless set of equations

$$\frac{\partial}{\partial t}w = \frac{\partial^2}{\partial x^2}w - V\frac{\partial}{\partial x}w + K(1-w), \quad x \in (0,1),\ t > 0, \tag{4}$$

$$-\frac{\partial}{\partial x}w(0,t) + Vw(0,t) = 0, \tag{5}$$

$$-\frac{\partial}{\partial x}w(1,t) + Vw(1,t) = -(1-n(t))B(A - w(1,t)), \tag{6}$$

where $n(t) \in \{0,1\}$ is a two-state Markov jump process that leaves state $n \in \{0,1\}$ at the dimensionless rate $\alpha_n > 0$. This model has the following 6 dimensionless parameters,

$$V := \frac{vL}{D_w} \leq 0, \quad K := \frac{kL^2}{D_w}, \quad B := \frac{bL}{D_w} = \frac{4L}{\pi a},$$
$$A := \frac{A_w}{I_w}, \quad \alpha_0 := \frac{\overline{\alpha}_0 L^2}{D_w}, \quad \alpha_1 := \frac{\overline{\alpha}_1 L^2}{D_w}. \tag{7}$$

Furthermore, it is sometimes convenient to work with the dimensionless overall opening/closing rate,

$$R := \frac{rL^2}{D_w} = \alpha_0 + \alpha_1. \tag{8}$$

Note that when $n(t) = 0$, the boundary condition at $x = 1$ is

$$-\frac{\partial}{\partial x}w(1,t) + Vw(1,t) = -B(A - w(1,t)). \tag{9}$$

Similarly, when $n(t) = 1$, the boundary condition at $x = 1$ is

$$-\frac{\partial}{\partial x}w(1,t) + Vw(1,t) = 0. \tag{10}$$

3 Probability distribution of the solution to the random PDE

In this section, we construct the random solution to (4)–(6), prove it converges in distribution at large time, and analyze this limiting distribution. In particular, we find

the support of this limiting distribution and find an explicit formula for this distribution in a certain parameter limit. The analysis in this section is similar to section 3 in Lawley and Keener (2019) which modeled electrodiffusion in a gated ion channel.

3.1 Construction of the solution

We construct the random solution to (4)–(6) by repeatedly composing the deterministic solution operators for open and closed boundary conditions. Let

$$\Phi_0^t : L^2[0,1] \to L^2[0,1]$$

denote the solution operator which takes an initial condition $f \in L^2[0,1]$ and maps it to the solution $\Phi_0^t(f)$ of the deterministic PDE (4) with fixed boundary conditions (5) and (9) at time $t > 0$. Similarly, let Φ_1^t denote the solution operator for (4) with fixed boundary conditions (5) and (10). These solution operators are given in Lemma 1 below.

We denote the standard $L^1[0,1]$ and $L^\infty[0,1]$ norms by $\|\cdot\|_1$ and $\|\cdot\|_\infty$ respectively. Define the weighted $L^2[0,1]$ inner product,

$$(f,g)_w := \int_0^1 f(x)g(x)e^{-Vx}\,\mathrm{d}x, \tag{11}$$

and the corresponding norm, $\|f\|_w := \sqrt{(f,f)_w}$. The inner product in (11) is chosen so that the spatial differential operators in (4) are self-adjoint.

Since we want to compute explicit formulas in various asymptotic limits, we need explicit formulas for Φ_0^t and Φ_1^t as well as their eigenfunctions and eigenvalues.

Lemma 1 *The solution operator, $\Phi_0^t : L^2[0,1] \to L^2[0,1]$, which takes an initial condition $f \in L^2[0,1]$, and maps it to the solution of (4) with boundary conditions (5) and (9) is*

$$(\Phi_0^t(f))(x) := w_0^{ss}(x) + \sum_{k=0}^{\infty} e^{-\mu_0^{(k)}t}\left(\phi_0^{(k)}, f - w_0^{ss}\right)_w \phi_0^{(k)}(x), \tag{12}$$

where $w_0^{ss}(x)$ is the steady-state solution of (4), (5), (9), the eigenvalues are

$$-\mu_0^{(k)} := -\left(\frac{V^2}{4} + \lambda_0^{(k)} + K\right) < 0, \quad k \geq 0,$$

where $\lambda_0^{(k)} > 0$ is the kth positive solution of the transcendental equation,

$$\tan\left(\sqrt{\lambda_0^{(k)}}\right) = \frac{B\sqrt{\lambda_0^{(k)}}}{V^2/4 - (V/2)B + \lambda_0^{(k)}}, \quad k \geq 1,$$

and the orthonormal (with respect to $(\cdot,\cdot)_w$) eigenfunctions are

$$\phi_0^{(k)}(x) := \nu_0^{(k)} e^{\frac{V}{2}x}\left[\frac{V}{2}\sin\left(\sqrt{\lambda_0^{(k)}}x\right) + \sqrt{\lambda_0^{(k)}}\cos\left(\sqrt{\lambda_0^{(k)}}x\right)\right], \quad k \geq 1,$$

where $\nu_0^{(k)}$ is such that $\|\phi_0^{(k)}\|_w = 1$. Furthermore, if $B(1+V/2) < V^2/4$, then $-\lambda_0^{(0)} \in (0, V^2/4)$ is the unique positive solution to

$$\tanh\left(\sqrt{-\lambda_0^{(0)}}\right) = \frac{B\sqrt{-\lambda_0^{(0)}}}{V^2/4 - (V/2)B + \lambda_0^{(0)}},$$

and

$$\phi_0^{(0)}(x) := \nu_0^{(0)} e^{\frac{V}{2}x}\left[\frac{V}{2}\sinh\left(\sqrt{-\lambda_0^{(0)}}x\right) + \sqrt{\lambda_0^{(0)}}\cosh\left(\sqrt{-\lambda_0^{(0)}}x\right)\right],$$

where $\nu_0^{(0)}$ is such that $\|\phi_0^{(0)}\|_w = 1$. If $B(1+V/2) \geq V^2/4$, then $\phi_0^{(0)}(x) \equiv 0$ and the value of $\lambda_0^{(0)}$ is irrelevant.

Similarly, the solution operator of (4) with boundary conditions (5) and (10) is

$$(\Phi_1^t(f))(x) := w_1^{ss}(x) + \sum_{k=0}^{\infty} e^{-\mu_1^{(k)}t}\left(\phi_k,\, f - w_1^{ss}\right)_w \phi_1^{(k)}(x), \tag{13}$$

where $w_1^{ss}(x)$ is the steady-state solution of (4), (5), (10), the eigenvalues are

$$-\mu_1^{(k)} := -\left(\frac{V^2}{4} + \lambda_1^{(k)} + K\right) < 0, \quad k \geq 0,$$

where $\lambda_1^{(0)} = -V^2/4$ and $\lambda_1^{(k)} = k^2\pi^2$ for $k \geq 1$, and the orthonormal (with respect to $(\cdot,\cdot)_w$) eigenfunctions are

$$\phi_1^{(0)}(x) := \nu_1^{(0)} e^{\frac{V}{2}x}\left[\sinh(\tfrac{V}{2}x) + \cosh(\tfrac{V}{2}x)\right] = \nu_1^{(0)} e^{Vx},$$
$$\phi_1^{(k)}(x) := \nu_1^{(k)} e^{\frac{V}{2}x}\left[\frac{V}{2}\sin(k\pi x) + k\pi\cos(k\pi x)\right], \quad k \geq 1,$$

where $\nu_1^{(k)}$ is such that $\|\phi_1^{(k)}\|_w = 1$ for $k \geq 0$.

We note that we can solve for the steady-states $w_0^{\mathrm{ss}}(x)$ and $w_1^{\mathrm{ss}}(x)$ explicitly, but the formulas are quite complicated so we collect them in the Appendix.

Proof of Lemma 1 Let $n \in \{0,1\}$. It is immediate that if $(\Phi_n^t(f))(x) = w_n^{\mathrm{ss}}(x) + h(x,t)$, then $h(x,0) = f(x) - w_n^{\mathrm{ss}}(x)$ and $h(x,t)$ satisfies the homogeneous problem,

$$\frac{\partial}{\partial t}h = \frac{\partial^2}{\partial x^2}h - V\frac{\partial}{\partial x}h - Kh, \quad x \in (0,1),\ t > 0,$$

$$-\frac{\partial}{\partial x}h(0,t) + Vh(0,t) = 0,$$
$$-\frac{\partial}{\partial x}h(1,t) + Vh(1,t) = (1-n)Bh(1,t).$$

Further, it is straightforward to check that if $h(x,t) = e^{-(\frac{V^2}{4}+K)t}e^{(\frac{V}{2})x}u(x,t)$, then $u(x,t)$ satisfies the diffusion equation with Robin boundary conditions,

$$\begin{aligned}\frac{\partial}{\partial t}u = \frac{\partial^2}{\partial x^2}u, \quad x \in (0,1),\ t > 0,\\ -\frac{\partial}{\partial x}u(0,t) + \frac{V}{2}u(0,t) = 0,\\ -\frac{\partial}{\partial x}u(1,t) + \frac{V}{2}u(1,t) = (1-n)Bu(1,t).\end{aligned}$$

Solving for $u(x,t)$ by a standard separation of variables calculation completes the proof. □

The solution of (4) with randomly switching boundary conditions (4)–(6) is then constructed by repeatedly composing Φ_0 and Φ_1 according to the Markov process $\{n(t)\}_{t\geq 0}$ (for similar constructions, see Lawley et al. 2015; Lawley 2018a; Lawley and Keener 2019). To describe this precisely, we need some more notation.

Let $\{\xi_k\}_{k=1}^{\infty}$ denote the sequence of states visited by $\{n(t)\}_{t\geq 0}$. Specifically, let $\xi_1 \in \{0,1\}$ be a Bernoulli random variable with mean $p_0 = \alpha_1/(\alpha_0+\alpha_1)$ and define $\xi_k = 1-\xi_{k-1}$ for $k \geq 2$. Next, let

$$\{s_k\}_{k=1}^{\infty} \tag{14}$$

be a sequence of independent exponential random variables with unit mean, $\mathbb{E}[s_k] = 1$. The sequence of dwell times of $\{n(t)\}_{t\geq 0}$ are then $\tau_k := s_k/\alpha_{\xi_k}$ for $k \geq 1$, and the kth switch happens at time

$$S_k := \sum_{i=1}^{k}\tau_i.$$

Define the number of jumps before time t,

$$N(t) := \sup\left\{k \in \mathbb{N}\cup\{0\} : S_k < t\right\},$$

and let $a(t) := t - S_{N(t)}$ be the time elapsed since the most recent jump. The random solution at time $t \geq 0$ is then the iterative random composition,

$$w(x,t) = \Phi^{a(t)}_{\xi_{N(t)+1}} \circ \Phi^{\tau_{N(t)}}_{\xi_{N(t)}} \circ \cdots \circ \Phi^{\tau_1}_{\xi_1}(w(x,0)). \tag{15}$$

3.2 Steady-state distribution of solution to random PDE

We now apply the mathematical methods developed in Lawley et al. (2015) to prove that $w(x,t)$ converges in distribution at large time and to analyze the limiting distribution. These methods require that the operators Φ_0^t and Φ_1^t in (15) are contracting in some average sense. The following lemma proves that these operators are in fact contracting almost surely in the weighted norm corresponding to the inner product in (11).

Lemma 2 *For each $n \in \{0,1\}$, there exists a constant $\zeta_n > 0$ so that for all $f, g \in L^2[0,1]$ and $t \geq 0$, we have the following bound,*

$$\|\Phi_n^t(f) - \Phi_n^t(g)\|_w \leq e^{-\zeta_n t}\|f - g\|_w.$$

Proof This lemma is a direct consequence of Lemma 1 and the fact that $\mu_n^{(k)} > 0$ for $n \in \{0,1\}$ and $k \geq 0$. □

Since Φ_0^t and Φ_1^t are contracting, the solution $w(x,t)$ defined in (15) must converge in distribution at large time. We need some more notation to describe the limiting distribution. Define the pair of compositions,

$$\Psi_n^{s,t} = \Phi_n^{s/\alpha_n} \circ \Phi_{1-n}^{t/\alpha_{1-n}}, \quad s,t \geq 0, \ n \in \{0,1\}.$$

For $\{s_k\}_{k=1}^{\infty}$ as in (14), define the pair of $L^2[0,1]$-valued random variables,

$$C_n := \lim_{j\to\infty} \Psi_n^{s_1,s_2} \circ \Psi_n^{s_3,s_4} \circ \cdots \circ \Psi_n^{s_{2j-1},s_{2j}}(f), \quad f \in L^2[0,1], \ n \in \{0,1\}, \quad (16)$$

which are termed random pullback attractors. In words, C_n takes an initial condition ($f \in L^2[0,1]$ in (16)) and "pulls it back" to the infinite past (Crauel 2001; Mattingly 1999; Schmalfuß 1996). Proposition 2.1 in Lawley et al. (2015) ensures that C_n exists almost surely as a limit in $L^2[0,1]$ since Lemma 2 implies that $\Psi_n^{s,t}$ is a contraction in $L^2[0,1]$ with the weighted norm $\|\cdot\|_w$ for all $s,t > 0$. We note that the convergence of this almost sure limit is in the weighted norm $\|\cdot\|_w$, but convergence in $\|\cdot\|_w$ is equivalent to convergence in $\|\cdot\|_2$. In addition, Proposition 2.1 in Lawley et al. (2015) ensures that C_n does not depend on the initial condition f in (16).

The steady state distribution of $w(x,t)$ is given in the following proposition, which is a direct consequence of Corollary 2.5 in Lawley et al. (2015).

Proposition 1 *Let $\eta \in \{0,1\}$ be a Bernoulli random variable with mean*

$$\mathbb{E}[\eta] = p_1 := \frac{\alpha_0}{\alpha_0 + \alpha_1}.$$

The following convergence in distribution holds,

$$(n(t), w(x,t)) \to_d (\eta, C(x)) \quad \text{as } t \to \infty,$$

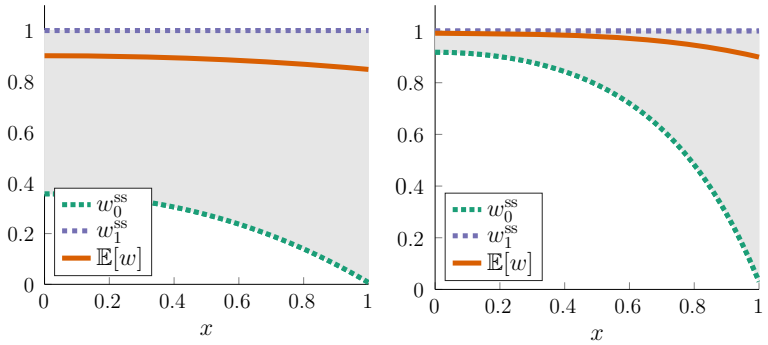

Fig. 1 At large time, the random solution $w(x,t)$ must lie in the gray region between the two deterministic steady states, w_0^{ss} (green dotted curve) and w_1^{ss} (purple dashed curve). The solid orange curve is the large time mean of w computed in Sect. 4. We take $K = 1$ in the left panel and $K = 10$ in the right panel. We take $V = A = 0$, $B = 100$, $\rho_0 = 0.2$, and $R = 1$ in both panels

where C is the following mixture of the random pullback attractors in (16),

$$C(x) = (1-\eta)C_0(x) + \eta C_1(x). \tag{17}$$

The pullback C_0 is the steady state random solution conditioned on the spiracle being open, and similarly C_1 is the steady state random solution conditioned on the spiracle being closed. Therefore, Proposition 1 states that the large-time distribution is given by C_η, where $\eta \in \{0, 1\}$ determines whether the spiracle is open or closed.

The following proposition gives the intuitive result that the limiting distribution of $w(x,t)$ is smooth and must be between the two deterministic steady states, w_0^{ss} and w_1^{ss}. This region between w_0^{ss} and w_1^{ss} is illustrated in Fig. 1.

Proposition 2 *For each $x \in [0,1]$, define*

$$w_-(x) := \min\{w_0^{ss}(x), w_1^{ss}(x)\},$$
$$w_+(x) := \max\{w_0^{ss}(x), w_1^{ss}(x)\}.$$

Define the set of smooth functions between w_0^{ss} and w_1^{ss},

$$S := \{g \in C^\infty[0,1] : w_-(x) \le g(x) \le w_+(x) \text{ for all } x \in [0,1]\}. \tag{18}$$

Then, $C(x) \in S$ almost surely, and $\Phi_n^t : S \to S$ for $n \in \{0,1\}$ and $t \ge 0$.

Proof Let $g \in S$. The function $\Phi_n^t(g)$ is infinitely differentiable in x if $t > 0$ since $\Phi_n^t(f)$ is infinitely differentiable in x for each $f \in L^2[0,1]$ and $t > 0$.

Let $u(x) := w_0^{ss}(x) - w_1^{ss}(x)$. It is immediate that u satisfies the following boundary value problem,

$$0 = u'' - Vu' - Ku, \quad x \in (0,1),$$
$$-u' + Vu = 0, \quad x = 0,$$

$$-u' + Vu = B(A - w_0^{\mathrm{ss}}(1)), \quad x = 1.$$

Solving this boundary value problem, we find that

$$u(x) = B(A - w_0^{\mathrm{ss}}(1))\frac{e^{\frac{1}{2}V(x-1)}}{2K}\operatorname{csch}\left(\frac{1}{2}\sqrt{4K+V^2}\right)\left[V\sinh\left(\frac{1}{2}x\sqrt{4K+V^2}\right)\right.$$
$$\left. + \sqrt{4K+V^2}\cosh\left(\frac{1}{2}x\sqrt{4K+V^2}\right)\right], \quad x \in [0,1]. \tag{19}$$

Therefore,

$$\operatorname{sgn}(w_0^{\mathrm{ss}}(x) - w_1^{\mathrm{ss}}(x)) = \operatorname{sgn}(B(A - w_0^{\mathrm{ss}}(1))), \quad x \in [0,1]. \tag{20}$$

where $\operatorname{sgn}(z)$ is the signum function.

Suppose $w_1^{\mathrm{ss}}(x) \geq w_0^{\mathrm{ss}}(x)$ for some $x \in (0,1]$, and thus $w_1^{\mathrm{ss}}(x) \geq w_0^{\mathrm{ss}}(x)$ for all $x \in (0,1]$ by (20). Observe that

$$\Phi_0^t(g)(x) - \Phi_0^t(w_0^{\mathrm{ss}})(x) = \Xi_0^t(g - w_0^{\mathrm{ss}})(x),$$

where Ξ_0^t is the solution operator for the homogeneous problem

$$\frac{\partial}{\partial t}v = \frac{\partial^2}{\partial x^2}v - V\frac{\partial}{\partial x}v - Kv, \quad x \in (0,1),\ t > 0, \tag{21}$$
$$-\frac{\partial}{\partial x}v(0,t) + Vv(0,t) = 0,$$
$$-\frac{\partial}{\partial x}v(1,t) + Vv(1,t) = Bv(1,t). \tag{22}$$

It is easy to check that Ξ_0^t satisfies the property that if $f \geq 0$, then $\Xi_0^t(f) \geq 0$. Therefore, if $g \in S$, then $g(x) - w_0^{\mathrm{ss}}(x) \geq 0$ for all $x \in [0,1]$, and thus $(\Phi_0^t(g))(x) \geq (\Phi_0^t(w_0^{\mathrm{ss}}))(x) = w_0^{\mathrm{ss}}(x)$ for all $x \in [0,1]$ and $t \geq 0$.

To check that $\Phi_0^t(g) \leq w_1^{\mathrm{ss}}$, consider the function

$$h(x,t) := w_1^{\mathrm{ss}}(x) - (\Phi_0^t(g))(x).$$

Then, h satisfies (21)–(22), with a nonnegative initial condition, $h(x,0) = w_1^{\mathrm{ss}}(x) - g(x) \geq 0$. Further, h satisfies

$$-\frac{\partial}{\partial x}h(1,t) + Vh(1,t) = B(A - (\Phi_0^t(g))(1)) \leq B(A - w_0^{\mathrm{ss}}(1)) \leq 0,$$

since $(\Phi_0^t(g))(x) \geq (\Phi_0^t(w_0^{\mathrm{ss}}))(x) = w_0^{\mathrm{ss}}(x)$ for all $x \in [0,1]$ and $t \geq 0$ and $B(A - w_0^{\mathrm{ss}}(1)) \leq 0$ by (20) and the assumption that $w_1^{\mathrm{ss}} \geq w_0^{\mathrm{ss}}$. Hence, $h(x,t) \geq 0$ for all $x \in [0,1]$ and $t \geq 0$, and therefore $\Phi_0^t : S \to S$.

The argument that $\Phi_1^t : S \to S$ is similar, and the case that $w_1^{\text{ss}} \leq w_0^{\text{ss}}$ is analogous. Since $\Phi_n^t : S \to S$ for $n \in \{0, 1\}$, Theorem 7 on page 24 of Lawley (2014) implies that $C_n \in S$ for $n \in \{0, 1\}$, and therefore $C \in S$. □

3.3 Almost sure limiting behavior

We now analyze the almost sure limiting behavior in the case that the overall opening/closing rate $R = \alpha_0 + \alpha_1 = rL^2/D_w$ is much slower than the water transfer rate $K = kL^2/D_w$,

$$\frac{\alpha_0 + \alpha_1}{K} = \frac{R}{K} = \frac{\overline{\alpha}_0 + \overline{\alpha}_1}{k} = \frac{r}{k} \ll 1. \tag{23}$$

Theorem 1 *Fix $p_0 \in (0, 1)$, $V \leq 0$, $B > 0$, and $A \geq 0$. If $n \in \{0, 1\}$, then*

$$\|C_n(x) - w_n^{\text{ss}}(x)\|_\infty \to 0 \quad \text{as} \quad \frac{\alpha_0 + \alpha_1}{K} \to 0 \quad \text{almost surely.}$$

Theorem 1 states that in the slow fluttering regime of (23), the pullbacks C_0 and C_1 converge to their corresponding steady states w_0^{ss} and w_1^{ss}. Since Proposition 1 gives the large time distribution of $w(x, t)$ as the Bernoulli mixture in (17) of C_0 and C_1, we have that the large time distribution of $w(x, t)$ in the regime of (23) is simply

$$(1 - \eta)w_0^{\text{ss}}(x) + \eta w_1^{\text{ss}}(x), \tag{24}$$

where $\eta \in \{0, 1\}$ is as in Proposition 1. Thus, (24) gives the full probability distribution of the random function $w(x, t)$ in the regime of (23).

Proof of Theorem 1 Define

$$g_{1-n} := \lim_{j \to \infty} \Phi_{1-n}^{s_2/\alpha_{1-n}} \circ \Psi_n^{s_3, s_4} \circ \cdots \circ \Psi_n^{s_{2j-1}, s_{2j}}(w_0^{\text{ss}}), \quad n \in \{0, 1\},$$

where $\{s_k\}_{k=1}^\infty$ are as in (14). Notice that g_{1-n} is defined so that $C_n = \Phi_n^{s_1/\alpha_n}(g_{1-n})$. Using Proposition 2, we have that

$$\begin{aligned}
\|C_n - w_n^{\text{ss}}\|_\infty &= \|\Phi_n^{s_1/\alpha_n}(g_{1-n}) - w_n^{\text{ss}}\|_\infty \\
&\leq e^{-(\frac{V^2}{4} + K)s_1/\alpha_n} \sum_{k=0}^{\infty} e^{-\lambda_n^{(k)} s_1/\alpha_n} |(\phi_n^{(k)}, g_{1-n} - w_n^{\text{ss}})_w| \|\phi_n^{(k)}\|_\infty \\
&\leq e^{-(\frac{V^2}{4} + K)s_1/\alpha_n} \|w_0^{\text{ss}} - w_1^{\text{ss}}\|_\infty \|e^{-Vx}\|_1 \sum_{k=0}^{\infty} e^{-\lambda_n^{(k)} s_1/\alpha_n} \|\phi_n^{(k)}\|_\infty^2.
\end{aligned} \tag{25}$$

Now, it is straightforward to check that the sum in (25) is convergent and independent of $\alpha_0 + \alpha_1$ and K. Furthermore, it is straightforward to check that $\|w_0^{\text{ss}}(x) - w_1^{\text{ss}}(x)\|_\infty$

is a bounded function of $K \in (0, \infty)$. Therefore, since $s_1 > 0$ almost surely, we see from (25) that taking $(\alpha_0 + \alpha_1)/K \to 0$ completes the proof. □

4 Mean solution and flux

The previous section focused on the probability distribution of the random solution. In this section, we study the mean solution and flux by applying the methods developed in Bressloff and Lawley (2015) and Lawley (2016).

4.1 Boundary value problem and solution

Define the pair of deterministic functions,

$$w_n(x,t) := \mathbb{E}[w(x,t)1_{n(t)=n}], \quad n \in \{0,1\},$$

where $1_{n(t)=n}$ is the indicator function,

$$1_{n(t)=n} = \begin{cases} 1 & \text{if } n(t) = n, \\ 0 & \text{if } n(t) \neq n. \end{cases}$$

Notice that mean solution is then given by

$$\mathbb{E}[w(x,t)] = w_0(x,t) + w_1(x,t). \tag{26}$$

Under the following regularity assumption,

$$\mathbb{E} \sup_{x\in[0,1]} \left|\tfrac{\partial}{\partial x} w(x,t)\right| < \infty, \quad \text{for each } t \geq 0,$$

Theorem 1 in Lawley (2016) ensures that w_0 and w_1 satisfy

$$\begin{aligned} \frac{\partial}{\partial t} w_0 &= \frac{\partial^2}{\partial x^2} w_0 - V \frac{\partial}{\partial x} w_0 + K(p_0 - w_0) - \alpha_0 w_0 + \alpha_1 w_1, \\ \frac{\partial}{\partial t} w_1 &= \frac{\partial^2}{\partial x^2} w_1 - V \frac{\partial}{\partial x} w_1 + K(p_1 - w_1) + \alpha_0 w_0 - \alpha_1 w_1, \end{aligned} \tag{27}$$

assuming $n(t)$ starts in its equilibrium distribution,

$$\mathbb{P}(n(0) = 0) = p_0 := \tfrac{\alpha_1}{\alpha_1+\alpha_0}, \quad \mathbb{P}(n(0) = 1) = p_1 := 1 - p_0.$$

In addition, w_0 and w_1 satisfy the following boundary conditions

$$\begin{aligned} -\frac{\partial}{\partial x} w_n(0,t) + V w_n(0,t) &= 0, \quad n \in \{0,1\}, \\ -\frac{\partial}{\partial x} w_0(1,t) + V w_0(1,t) &= -B(p_0 A - w_0(1,t)), \\ -\frac{\partial}{\partial x} w_1(1,t) + V w_1(1,t) &= 0. \end{aligned} \tag{28}$$

To explain (27)–(28) in words, the time evolution of w_n in (27) is identical to that of w in (4) except for two differences. First, (27) contains reaction terms, $-\alpha_n w_n + \alpha_{1-n} w_{1-n}$, which describe the flow of probability out of and in to state $n \in \{0, 1\}$. Second, the inhomogeneous term K in (4) is weighted by p_n in (27), where p_n is the equilibrium probability that $n(t) = n$. Further, the boundary conditions in (28) for w_n are identical to those for w in (5)–(6) when $n(t) = n$, except the inhomogeneous term BA in (6) is weighted by p_n in (28). We note that if we did not assume that $n(t)$ starts in its invariant distribution, then p_n in (27)–(28) would merely be replaced by the function of time,

$$\mathbb{P}(n(t) = n) = p_n + e^{-(\alpha_0+\alpha_1)t}\big(\mathbb{P}(n(0) = n) - p_n\big),$$

which converges exponentially fast to p_n as time increases. Summarizing, the mean solution in (26) can be found by solving the deterministic boundary value problem in (27)–(28).

The large-time mean flux at $x = 1$,

$$W_{\text{flutter}} := \lim_{t\to\infty} \Big[-\frac{\partial}{\partial x}(w_0 + w_1) + V(w_0 + w_1) \Big]\Big|_{x=1},$$

can be written as

$$W_{\text{flutter}} = f_w(p_0, \alpha_0 + \alpha_1, K, V, B) W_{\text{open}}, \tag{29}$$

where W_{open} is the flux when the spiracle is always open,

$$W_{\text{open}} := \Big[-\frac{\partial}{\partial x} w_0^{\text{ss}} + V w_0^{\text{ss}} \Big]\Big|_{x=1},$$

and

$$f_w = f_w(p_0, \alpha_0 + \alpha_1, K, V, B) \in (p_0, 1)$$

is a dimensionless factor that describes how fluttering reduces the flux compared to always being open. We refer to f_w as the *water flutter factor*. Solving the boundary value problem (27)–(28) at steady state, we can find explicit formulas for W_{flutter}, W_{open}, and f_w. However, these formulas are very complicated and so we relegate them to the Appendix.

4.2 Limiting behavior of mean solution and flux

We now investigate the behavior of the mean flux in various parameter limits using the explicit formulas for f_w, W_{flutter}, and W_{open} given in the Appendix. We first note that

$$\lim_{p_0 \to 0} f_w = 0.$$

This is expected, since this merely states that if the spiracle is never open ($p_0 = 0$), then there is no water loss. Similarly, if the spiracle is always open ($p_0 = 1$), then W_{flutter} is the same as W_{open},

$$\lim_{p_0 \to 1} f_w = 1.$$

If $K \to 0$, then there is no water loss,

$$\lim_{K \to 0} W_{\text{flutter}} = \lim_{K \to 0} W_{\text{open}} = 0, \tag{30}$$

and the formula for f_w in the Appendix implies $\lim_{K \to 0} f_w = 1$. Furthermore,

$$\lim_{K \to \infty} f_w = \lim_{V \to -\infty} f_w = \lim_{\alpha_0 + \alpha_1 \to 0} f_w = p_0.$$

5 Physiological implications

In this section, we investigate the physiological implications of our mathematical model. The model depends in a complicated way on 6 dimensionless parameters, namely p_0, R, V, B, A, and K (see (7)–(8) for parameter definitions). We thus begin by estimating these parameters.

Recall that $B = 4L/(\pi a)$ is a geometric parameter that compares the length of a tracheal tube, $L > 0$, to its radius $a > 0$. The trachea of most insects are long and thin, and indeed we estimate below (see Table 1) that the aspect ratio is typically in the range

$$\frac{a}{L} \in [0.002, 0.05]. \tag{31}$$

Therefore, for simplicity we set $B = \infty$ in our calculations in this section, though we note that using finite values of B corresponding to the range of a/L in (31) would have little effect on our results.

While convection is known to play a role during the flutter phase (Lighton 1996b), the relative importance of convection and diffusion is debated (Chown et al. 2006). For simplicity, we therefore ignore convection in this section by setting $V = 0$ in our calculations (recall that V is the dimensionless convective velocity). Our main result is that during the flutter phase water loss is approximately proportional to the percentage

Table 1 Estimates of tracheal length $L > 0$, tracheal radius $a > 0$, percentage of time open during the flutter phase $p_0 \in (0, 1)$, flutter rate $r = \overline{\alpha}_0 + \overline{\alpha}_1 > 0$, and water transfer rate $k > 0$ for several types of insects

Insect	L (cm)	a (cm)	p_0	r (1/s)	k (1/s)
Giant saturniid silkworms	1		0.09	2.2	
Cataglyphis bicolor	0.38		0.2	24	
Gromphadorhina portentosa	1.6		0.28	2.33	
Pine weevil	0.3		0.2	0.1	
Rhodnius	0.25	0.002			$\geq 3.8 \times 10^4$
Flea	0.05	0.0025			≥ 341
Mealworm	0.15	0.005			≥ 7.7

The values in the first 4 rows were estimated in Lawley et al. (2020). The values in the final 3 rows are estimated in Sect. 5.1 using data from Wigglesworth and Gillett (1936) and Mellanby (1934)

of time the spiracles are open, which means that fluttering conserves water. Since the convective flow of air during the flutter phase is inward, it is clear that including convection in our analysis would only strengthen this result.

By taking $B = \infty$ and $V = 0$, we obtain the following relatively simple formula for the water flutter factor in (29),

$$f_w^0 := \lim_{V\to 0} \lim_{B\to\infty} f_w = \left(1 + \frac{1-p_0}{p_0} \frac{\sqrt{K}\tanh\sqrt{K}}{\sqrt{R+K}\tanh\sqrt{R+K}}\right)^{-1} \in (p_0, 1), \quad (32)$$

which depends on the 3 dimensionless parameters, p_0, R, and K (f_w is independent of the parameter A describing the ambient water concentration since W_{flutter} and W_{open} are each proportional to $1 - A$). Recall that $p_0 \in (0, 1)$ is the percentage of time the spiracles are open during the flutter phase, $R = rL^2/D_w > 0$ compares the fluttering rate $r = \overline{\alpha}_0 + \overline{\alpha}_1$ to the diffusion timescale L^2/D_w, and $K = kL^2/D_w > 0$ compares the water transfer rate k to the diffusion timescale. The formula in (32) appeared in an equivalent form in our previous work (Lawley et al. 2020). In previous work, we estimated p_0 and R for different insects and we give these values in the first 4 rows of Table 1. It therefore remains to estimate the water transfer rate k to estimate $K = kL^2/D_w$.

5.1 Estimating the water transfer rate *k*

Wigglesworth and Gillett (1936) and Mellanby (1934) measured the rate of water loss from insects that are forced to keep their spiracles permanently open. We now use this data to estimate the water transfer rate k.

In the case that the spiracle is always open, the steady-state, dimensionless flux of water vapor out of the spiracle is

$$W_{\text{open}} = \sqrt{K}\tanh(\sqrt{K}), \quad (33)$$

where we have set $A = 0$, since the data in Wigglesworth and Gillett (1936); Mellanby (1934) is for insects in dry air. To get (33) into units of (mass of water) per (time × area), we recall the scalings in Sect. 2.2 and therefore multiply W_{open} by $I_w D_w / L$. Taking seconds as our time unit, we then obtain the mass of water lost per hour by multiplying by (i) the cross-sectional area of a tracheal tube, πa^2, (ii) the number of spiracles on an insect, n_{spir}, and (iii) the number of seconds in an hour, 60^2. Thus,

$$\mathcal{L} := \text{mass of water lost per hour} = \sqrt{K}\tanh(\sqrt{K})\frac{I_w D_w}{L}\pi a^2 n_{\text{spir}} 60^2. \tag{34}$$

We take $D_w = 0.282\,\text{cm}^2/\text{s}$ (Cussler 2009) and set $n_{\text{spir}} = 20$ which is typical for most insects. The parameter I_w is difficult to estimate, but since it is a water vapor concentration, it has a maximum value. In particular, we have that $I_w \leq 2.3 \times 10^{-2}\,\text{mg/cm}^3$ at 24 degrees Celsius. By using this maximum value for I_w and experimentally measured values of $\mathcal{L}$, we can use (34) to obtain lower bounds for K.

Wigglesworth and Gillett (1936) found that *Rhodnius* loses 13 milligrams of water per day when forced to keep its spiracles open, which yields $\mathcal{L} \approx 0.54\,\text{mg/h}$ in (34). For *Rhodnius*, we estimate a tracheal radius of $a = 0.001\,\text{cm}$ and tracheal length of $L = 0.25\,\text{cm}$. We thus obtain the following lower bound for *Rhodnius* from (34),

$$k \geq 3.8 \times 10^4\,\text{s}^{-1}. \tag{35}$$

In similar experiments, Mellanby (1934) found that a flea loses $\mathcal{L} = 0.3\,\text{mg/h}$ of water. For fleas, we estimate that $a = 0.0025\,\text{cm}$ and $L = 0.05\,\text{cm}$, and thus (34) implies the following lower bound for fleas,

$$k \geq 341\,\text{s}^{-1}. \tag{36}$$

In addition, Mellanby (1934) found that a mealworm loses $\mathcal{L} = 0.125\,\text{mg/h}$ of water. For mealworms, we estimate that $a = 0.005\,\text{cm}$ and $L = 0.15\,\text{cm}$, and thus (34) implies the following lower bound for mealworms,

$$k \geq 7.7\,\text{s}^{-1}. \tag{37}$$

5.2 Fluttering conserves water

Before using our lower bounds for k and $K = kL^2/D_w$, recall that if $K \ll 1$, then our analysis in Sect. 4 shows that respiratory water loss is negligible (see 30). Therefore, respiratory water loss threatens an insect only if K is not very small. In the limit of large K, it follows from (32) that

$$\lim_{K\to\infty} f_w^0 = p_0. \tag{38}$$

This means that an insect can restrict water loss by keeping its spiracles open only a small percentage of time (small p_0) in the case that respiratory water loss is a significant threat (large K).

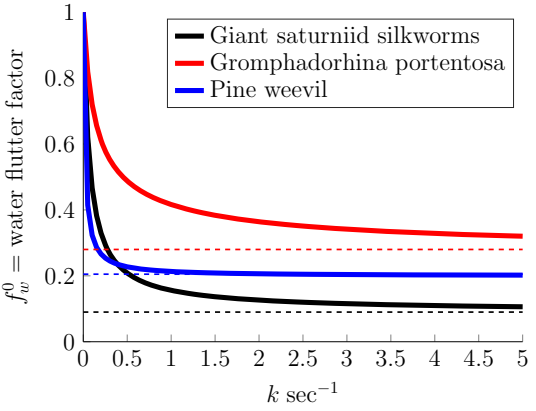

Fig. 2 Simplified water flutter factor f_w^0 in (32) as a function of water transfer rate k for 3 types of insects

However, to see if a particular insect is in the regime of $f_w^0 \approx p_0$, one has to consider how the flutter rate compares to the water transfer rate. Indeed, if we define the ratio of these rates,

$$\beta := \frac{R}{K} = \frac{r}{k} > 0, \tag{39}$$

then a direct calculation with (32) yields

$$\begin{aligned} \lim_{\beta \to 0} f_w^0 &= p_0, \\ \lim_{\beta \to \infty} f_w^0 &= 1. \end{aligned} \tag{40}$$

Unfortunately, we are not able to directly estimate β for a specific insect since our estimates of r and our estimates of k come from two different sets of insects (see Table 1). However, since the estimates of r are generally much smaller than the estimates of k, it is likely that most insects are in the regime $f_w^0 \approx p_0$ of (40). We now investigate this in more detail.

In Fig. 2, we plot the water flutter factor f_w^0 as a function of k for 3 insects for which we have estimates of flutter rates. For these insects, we see that f_w^0 rapidly decreases from 1 to p_0 as k increases, with $f_w^0 \approx p_0$ as long as $k \geq 5\,\mathrm{s}^{-1}$. While we do not have estimates of k that are specific to these insects, since our estimates of k in (35)–(37) (which are actually lower bounds) range from $7.7\,\mathrm{s}^{-1}$ to more than $10^4\,\mathrm{s}^{-1}$, the flutter factors for these insects are likely very close to p_0.

Furthermore, using our estimates in (35)–(37) for *Rhodnius*, fleas, and mealworms, it follows from (32) that the flutter factors for these insects are very close to p_0, as long as their flutter rates are not too large. Indeed, if we take the largest estimated flutter rate of $r = 24\,\mathrm{s}^{-1}$, then the flutter factors for *Rhodnius*, fleas, and mealworms all satisfy $f_w^0 - p_0 < 0.02$ for $p_0 = 0.2$. Taking smaller flutter rates only make f_w^0 closer to p_0.

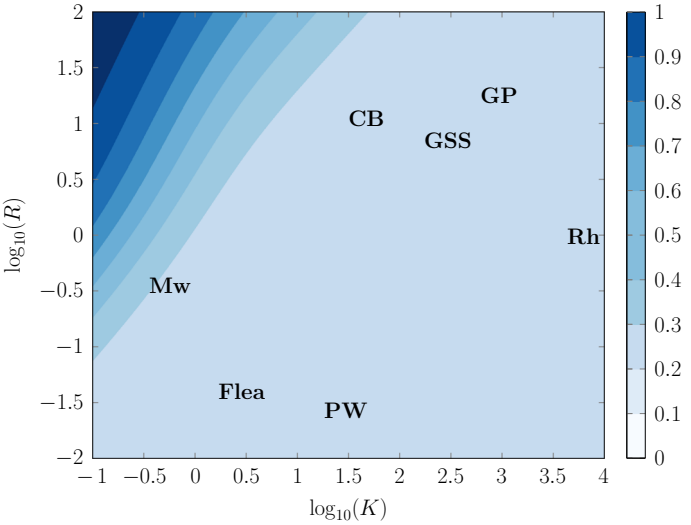

Fig. 3 Simplified water flutter factor f_w^0 as a function of $K = kL^2/D_w$ and $R = rL^2/D_w$ for $p_0 = 0.2$. The 7 insects (Giant saturniid silkworm (GSS), Cataglyphis bicolor (CB), Gromphadorhina portentosa (GP), Pine weevil (PW), Rhodnius (Rh), flea, mealworm (Mw)) are placed according to their estimates of k, L, and r

In Fig. 3, we plot f_w^0 as a function of $R = rL^2/D_w$ and $K = kL^2/D_w$ for $p_0 = 0.2$ and place the 7 insects of Table 1 in this two-dimensional parameter space. Since we only have flutter rate data for 4 insects, we take $r = 5\,\mathrm{s}^{-1}$ for the other 3 insects for this figure. Similarly, since we only have water loss data for 3 insects, we set $k = 100\,\mathrm{s}^{-1}$ for the other 4 insects for this figure. Notice that all 7 insects are in the region with $f_w^0 \approx p_0$. Taking smaller values of r and larger values of k would make f_w^0 even closer to p_0. Summarizing, our analysis predicts that $f_w^0 \approx p_0$ for the 7 insects in Table 1.

5.3 Fluttering decouples water loss and oxygen uptake

In previous work (Lawley et al. 2015, 2020), we formulated and analyzed a model of oxygen uptake during the flutter phase. We defined the oxygen flutter factor, f_{oxy}, as the ratio of the average oxygen uptake during the flutter phase, U_{flutter}, to the average oxygen uptake during the open phase, U_{open}, and found the following formula

$$f_{\mathrm{oxy}} := \frac{U_{\mathrm{flutter}}}{U_{\mathrm{open}}} = \left(1 + \frac{1-p_0}{p_0} \frac{\tanh\sqrt{R\frac{D_w}{D_o}}}{\sqrt{R\frac{D_w}{D_o}}}\right)^{-1} \in (p_0, 1),$$

where $D_o = 0.176\,\mathrm{cm}^2/\mathrm{s}$ is the diffusion coefficient of oxygen (Cussler 2009).

For about 200 different species, Woods and Smith (2010) looked at the ratio, $\rho > 0$, of water loss to oxygen uptake. For our model, this ratio during the open phase is

$$\rho_{\text{open}} = \frac{W_{\text{open}}}{U_{\text{open}}},$$

and during the flutter phase, this ratio is

$$\rho_{\text{flutter}} = \frac{W_{\text{flutter}}}{U_{\text{flutter}}}.$$

To investigate the ability of fluttering to decouple water loss from oxygen uptake, we define

$$\Sigma := \frac{\rho_{\text{flutter}}}{\rho_{\text{open}}} = \frac{f_w^0}{f_{\text{oxy}}} \in (p_0, 1/p_0).$$

Notice that a decoupling of water loss and oxygen uptake in the flutter phase compared to the open phase corresponds to $\Sigma \neq 1$. Further, conserving water and maintaining a high oxygen uptake corresponds to making Σ small.

Using the formulas above and that $D_w/D_o \approx 1.6$, the ratio Σ is

$$\Sigma = \Sigma(p_0, R, K) = \frac{1 + \frac{1-p_0}{p_0} \frac{\tanh \sqrt{1.6R}}{\sqrt{1.6R}}}{1 + \frac{1-p_0}{p_0} \frac{\sqrt{K} \tanh \sqrt{K}}{\sqrt{R+K} \tanh \sqrt{R+K}}}. \tag{41}$$

In Fig. 4, we plot Σ as a function of the flutter rate r for different values of the water transfer rate k. The squares in Fig. 4 indicate the physiological values of r from Table 1. Notice that Σ is a non-monotonic function of the flutter rate. Further, while larger values of k require larger values of r to exactly minimize the ratio Σ, notice that taking $r \in [2, 24]\,\text{s}^{-1}$ yields values of Σ which are (i) far from the case that water loss and oxygen uptake are perfectly coupled (i.e. the case $\Sigma = 1$) and (ii) not far from the minimal values of Σ.

Summarizing, from the perspective of simply increasing oxygen uptake during the flutter phase, an insect is always better off by fluttering faster. However, if an insect needs to balance a high oxygen uptake and low water loss, then there is an optimal fluttering rate which minimizes Σ.

6 Discussion

As in all mathematical models of biological systems, we made various simplifying assumptions to make the problem tractable. We assumed that the tracheal cross-section is approximately constant as a function of depth in the trachea. We assumed that the waiting times for switching boundary conditions are exponentially distributed. We assumed a relatively simple no-flux boundary condition for water vapor at the

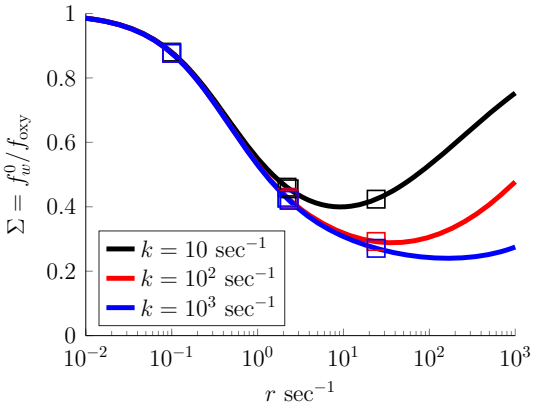

Fig. 4 Ratio $\Sigma = f_w^0/f_{\text{oxy}}$ as a function of flutter rate r for different values of the water transfer rate k with $p_0 = 0.2$. The squares are at the physiological estimates of r in Table 1

tracheoles. Making more detailed and complicated assumptions would almost certainly not change the main conclusion that water loss during the flutter phase is approximately proportional to the percentage of time open. Since oxygen uptake can be altered by the rate of fluttering this shows that water loss and oxygen uptake are effectively decoupled by fluttering.

We use stochastic methods because it is known that the lengths of open and closed bouts during the flutter phase vary considerably (Schneiderman 1960; Heinrich et al. 2013). Our model consists of a one-dimensional diffusion-convection equation with a stochastically switching boundary condition corresponding to "open" and "closed." After non-dimensionalizing, we obtained a PDE with six non-dimensional parameters. Using the techniques in (Lawley et al. 2015; Lawley 2016) we computed the probability distribution of the long-time solution and from that solution calculated an explicit formula for the expected water loss as a function of the six parameters. The explicit formula allowed us to calculate simpler formulas in asymptotic limits where various parameters became large and small. Finally, we used experimental data from various insects to estimate the ranges of the six parameters and this allowed us to conclude that in the flutter phase, water loss is approximately proportional to the percentage of time open. The calculations were long because of the need to derive explicit formulas for water loss in terms of the parameters.

PDEs with stochastically switching boundary conditions have been used to model a variety of other biological systems, including volume transmission in the brain (Lawley 2018b), the electrodiffusive flux of ions through a gated ion channel (Lawley and Keener 2019), and intercellular communication through gap junctions (Bressloff et al. 2020). A class of models which are mathematically similar and are also used to describe various biological systems are PDEs with stochastically switching righthand sides. For example, Klimasara et al. (2021) analyzed switching Liouville equations modeling population dynamics and gene expression. In addition, the diffusion equation with a switching diffusion coefficient has been used to model protein gradient formation in a zygote (Wu et al. 2018; Bressloff et al. 2019). Indeed, a variety of systems in cell biology involve molecules whose diffusivities fluctuate (Weron et al. 2017; Sungkaworn et al. 2017) and several statistical methods have been developed

to detect changes in diffusivity from particle tracking data (Das et al. 2009; Koo and Mochrie 2016; Monnier 2013; Montiel et al. 2006; Persson et al. 2013; Slator and Burroughs 2018; Slator et al. 2015). More generally, stochastically switching PDEs are an example of a piecewise deterministic Markov process (Davis 1984), whose applications in biology have been recently reviewed by Bressloff (2017), Cloez et al. (2017) and Rudnicki and Tyran-Kamińska (2017).

Oxygen uptake and water loss have been important issues in insect physiology for nearly a century since the pioneering work of Wigglesworth (Wigglesworth 1931; Wigglesworth and Gillett 1936; Wigglesworth 1965). When the spiracles are open, oxygen can diffuse in and carbon dioxide can diffuse out of the trachea, but water can also diffuse out, which is a serious problem for insects since the surface area of the tracheal trees is very large. When the spiracles are closed, there is no oxygen uptake or water loss from the respiratory system. Many insects, particularly those that live in dry environments or have little access to water, show a third dynamical state called fluttering in which they keep their spiracles closed a high percentage of time while also opening and closing rapidly for brief periods of time (Wigglesworth 1931; Schneidermann 1956; Contreras et al. 2014). In Lawley et al. (2020) we used the mathematical analysis in Lawley et al. (2015) to show that, no matter how small the percentage of time open, the insect could absorb oxygen almost as fast as if the spiracle were open 100% of the time if it flutters fast enough. And, we explained the intuition behind this surprising result and gave examples from specific insects.

Those results left open an important question, what happens to water loss during the flutter phase, the question we addressed in this paper. We have shown that, in parameter regimes corresponding to real insects, water loss during the flutter phase is approximately proportional to the percentage of time open. This means that during the flutter phase insects can achieve high oxygen intake and low water loss by keeping the spiracles closed a high percentage of time and fluttering rapidly. If insects switch between open and closed on a long time scale, then more oxygen uptake is the same as more water loss. Our results show that fluttering decouples oxygen uptake and water loss, and so insects can balance oxygen needs with energy expenditure independent of water loss. This is almost certainly the reason for fluttering.

7 Appendix

7.1 Formulas for w_0^{ss} and w_1^{ss}

Using Mathematica, it is straightforward to find that $w_0^{ss}(x) = \nu_0/\delta_0$, where

$$\begin{aligned}\nu_0 = 2e^{\frac{1}{2}\left((3-2x)\sqrt{4K+V^2}-V\right)}\Bigg(B\Bigg(&2(A-1)Ke^{\frac{1}{2}\left((3x-2)\sqrt{4K+V^2}+Vx\right)}\\&+(A-1)\left(-V\sqrt{4K+V^2}+2K+V^2\right)e^{\frac{1}{2}\left((x-2)\sqrt{4K+V^2}+Vx\right)}\\&+V\left(\sqrt{4K+V^2}-V\right)\exp\left(\frac{1}{2}\left(3(x-1)\sqrt{4K+V^2}+V(x+1)\right)\right)\end{aligned}$$

$$
\begin{aligned}
&+2Ke^{\frac{1}{2}\left((2x-1)\sqrt{4K+V^2}+V\right)}\\
&-V\left(\sqrt{4K+V^2}-V\right)e^{\frac{1}{2}\left((x-1)\sqrt{4K+V^2}+V(x+1)\right)}\\
&+\left(-V\sqrt{4K+V^2}+2K+V^2\right)e^{\frac{1}{2}\left((2x-3)\sqrt{4K+V^2}+V\right)}\Big)\\
&-2KV\exp\left(\frac{1}{2}\left(3(x-1)\sqrt{4K+V^2}+V(x+1)\right)\right)\\
&+2KVe^{\frac{1}{2}\left((3x-2)\sqrt{4K+V^2}+Vx\right)}\\
&+V\left(-V\sqrt{4K+V^2}+2K+V^2\right)e^{\frac{1}{2}\left((x-2)\sqrt{4K+V^2}+Vx\right)}\\
&-V\left(-V\sqrt{4K+V^2}+2K+V^2\right)e^{\frac{1}{2}\left((x-1)\sqrt{4K+V^2}+V(x+1)\right)}\\
&-K\left(\sqrt{4K+V^2}-V\right)e^{\frac{1}{2}\left((2x-3)\sqrt{4K+V^2}+V\right)}\\
&+K\left(\sqrt{4K+V^2}-V\right)e^{\frac{1}{2}\left((2x-1)\sqrt{4K+V^2}+V\right)}\Big),
\end{aligned}
$$

and

$$
\begin{aligned}
\delta_0=&\left(\sqrt{4K+V^2}-V\right)\left(B\left(\sqrt{4K+V^2}+e^{\sqrt{4K+V^2}}\left(\sqrt{4K+V^2}+V\right)\right)\right.\\
&\left.-BV+2K\left(e^{\sqrt{4K+V^2}}-1\right)\right).
\end{aligned}
$$

Furthermore, $w_1^{\mathrm{ss}}(x)=\nu_1/\delta_1$, where

$$
\begin{aligned}
\nu_1=e^{-\frac{V}{2}}&\left(-2KVe^{\frac{1}{2}\left(x\sqrt{4K+V^2}+Vx+V\right)}+2KVe^{\frac{1}{2}\left((x+1)\sqrt{4K+V^2}+Vx\right)}\right.\\
&+V\left(V\left(V-\sqrt{4K+V^2}\right)+2K\right)e^{\frac{1}{2}\left(Vx-(x-1)\sqrt{4K+V^2}\right)}\\
&-V\left(V\left(V-\sqrt{4K+V^2}\right)+2K\right)e^{\frac{1}{2}\left(V(x+1)-(x-2)\sqrt{4K+V^2}\right)}\\
&\left.-Ke^{V/2}\left(\sqrt{4K+V^2}-V\right)+Ke^{\sqrt{4K+V^2}+\frac{V}{2}}\left(\sqrt{4K+V^2}-V\right)\right),
\end{aligned}
$$

and

$$
\delta_1=K\left(e^{\sqrt{4K+V^2}}-1\right)\left(\sqrt{4K+V^2}-V\right).
$$

In the case that $V=0$, these expressions simplify to $w_1^{\mathrm{ss}}(x)=1$ and $w_0^{\mathrm{ss}}(x)=\nu_0'/\delta_0'$, where

$$\nu_0' = e^{-\sqrt{K}(x+1)}\left(B\left((A-1)e^{\sqrt{K}(2x+1)} + (A-1)e^{\sqrt{K}} + e^{\sqrt{K}x} + e^{\sqrt{K}(x+2)}\right)\right.$$
$$\left. + \left(e^{2\sqrt{K}} - 1\right)\sqrt{K}e^{\sqrt{K}x}\right),$$

and

$$\delta_0' = 2\left(B\cosh\left(\sqrt{K}\right) + \sqrt{K}\sinh\left(\sqrt{K}\right)\right).$$

7.2 Expected water flux formulas

Solving the boundary value problem (27)–(28) at steady state explicitly yields that the water flutter factor is given by $f_w = \nu/\delta$, where

$$\begin{aligned}
\nu = {} & p_0(K+r)\left(V\left(e^{\sqrt{4K+V^2}} - 1\right)\right. \\
& \left. + \left(e^{\sqrt{4K+V^2}} - 2e^{\frac{1}{2}\left(\sqrt{4K+V^2}+V\right)} + 1\right)\sqrt{4K+V^2}\right)\left(2BK\left(e^{\sqrt{4K+V^2}} + 1\right)\right. \\
& \left. + BV\left(V - \sqrt{4K+V^2}\right) + K\left(e^{\sqrt{4K+V^2}} - 1\right)\left(\sqrt{4K+V^2} - V\right)\right) \\
& \times e^{\frac{1}{2}\left(-\sqrt{4(K+r)+V^2} - \sqrt{4K+V^2}\right)}\left(e^{\sqrt{4(K+r)+V^2}} - 1\right), \\
\delta = {} & 4\left(2K\left(e^{\sqrt{4K+V^2}} - 2e^{\frac{1}{2}\left(\sqrt{4K+V^2}+V\right)} + 1\right)\right. \\
& \left. + V\left(e^{\frac{1}{2}\left(\sqrt{4K+V^2}+V\right)} - 1\right)\left(\sqrt{4K+V^2} - V\right)\right) \\
& \times \left(\sinh\left(\frac{1}{2}\sqrt{4(K+r)+V^2}\right)\left(\sinh\left(\frac{1}{2}\sqrt{4K+V^2}\right)(BKV + Bp_0rV\right.\right. \\
& \left. + 2K(K+r)) + Bp_0(K+r)\sqrt{4K+V^2}\cosh\left(\frac{1}{2}\sqrt{4K+V^2}\right)\right) \\
& - BK(p_0-1)\sqrt{4(K+r)+V^2}\sinh\left(\frac{1}{2}\sqrt{4K+V^2}\right) \\
& \left. \times \cosh\left(\frac{1}{2}\sqrt{4(K+r)+V^2}\right)\right).
\end{aligned}$$

References

Bezrukov SM, Berezhkovskii AM, Pustovoit MA, Szabo A (2000) Particle number fluctuations in a membrane channel. J Chem Phys 113(18):8206–8211

Bressloff PC (2017) Stochastic switching in biology: from genotype to phenotype. J Phys A 50(13):133001

Bressloff PC, Lawley SD (2015) Moment equations for a piecewise deterministic PDE. J Phys A. https://doi.org/10.1088/1751-8113/48/10/105001

Bressloff PC, Lawley SD (2016) Diffusion on a tree with stochastically gated nodes. J Phys A 49(24):245601

Bressloff PC, Lawley SD, Murphy P (2019) Protein concentration gradients and switching diffusions. Phys Rev E 99(3):032409

Bressloff PC, Lawley SD, Murphy P (2020) Effective permeability of a gap junction with age-structured switching. SIAM J Appl Math 80(1):312–337
Buck J, Keister M, Specht H (1953) Discontinuous respiration in diapausing agapema pupae. Anat Rec 117:541–541
Chown SL, Gibbs AG, Hetz SK, Klok CJ, Lighton JR, Marais E (2006) Discontinuous gas exchange in insects: a clarification of hypotheses and approaches. Physiol Biochem Zool 79(2):333–343. https://doi.org/10.1086/499992
Cloez B, Dessalles R, Genadot A, Malrieu F, Marguet A, Yvinec R (2017) Probabilistic and piecewise deterministic models in biology. ESAIM Proc Surv 60:225–245
Contreras HL, Heinrich EC, Bradley TJ (2014) Hypotheses regarding the discontinuous gas exchange cycle (DGC) of insects. Curr Opin Insect Sci 4:48–53
Crauel H (2001) Random point attractors versus random set attractors. J London Math Soc (2) 63(2):413–427. https://doi.org/10.1017/S0024610700001915
Cussler EL (2009) Diffusion: mass transfer in fluid systems. Cambridge University Press
Das R, Cairo CW, Coombs D (2009) A hidden Markov model for single particle tracks quantifies dynamic interactions between LFA-1 and the actin cytoskeleton. PLoS Comput Biol 5(11):e1000556
Davis MH (1984) Piecewise-deterministic Markov processes: a general class of non-diffusion stochastic models. J R Stat Soc Ser B (Methodol) 46(3):353–376
Heinrich E, McHenry M, Bradley T (2013) Coordinated ventilation and spiracle activity produce unidirectional airflow in the hissing cockroach, gromphadorhina portentosa. J Exp Biol 216:4473–4482
Klimasara P, Mackey MC, Tomski A, Tyran-Kamińska M (2021) Randomly switching evolution equations. Nonlinear Anal Hybrid Syst 39:100948
Koo PK, Mochrie SGJ (2016) Systems-level approach to uncovering diffusive states and their transitions from single-particle trajectories. Phys Rev E 94(5):052412
Krogh A (1920) Studien über Tracheenrespiration II: Über gasdiffusion in den tracheen. Pflüg Arch ges Physiol 179(1):95–112, https://doi.org/10.1007/BF01722125
Lawley SD (2014) Stochastic switching in evolution equations. PhD Thesis, Duke University
Lawley SD (2016) Boundary value problems for statistics of diffusion in a randomly switching environment: PDE and SDE perspectives. SIAM J Appl Dyn Syst 15:1410–1433
Lawley SD (2018) Blowup from randomly switching between stable boundary conditions for the heat equation. Commun Math Sci 16(4):1131–1154
Lawley SD (2018) A probabilistic analysis of volume transmission in the brain. SIAM J Appl Math 78(2):942–962
Lawley SD, Keener JP (2019) Electrodiffusive flux through a stochastically gated ion channel. SIAM J Appl Math 79(2):551–571
Lawley SD, Mattingly JC, Reed MC (2015) Stochastic switching in infinite dimensions with applications to random parabolic PDE. SIAM J Math Anal 47(4):3035–3063. https://doi.org/10.1137/140976716
Lawley SD, Reed MC, Nijhout HF (2020) Spiracular fluttering increases oxygen uptake. PLoS One 15(5):e0232450
Lighton J (1996) Discontinuous gas exchange in insects. Annu Rev Entomol 41(1):309–324. https://doi.org/10.1146/annurev.en.41.010196.001521
Lighton JRB (1996) Discontinuous gas exchange in insects. Annu Rev Entomol 41:309–324
Locke M (1958) The co-ordination of growth in the tracheal system of insects. J Cell Sci s3–99(47):373–391
Marias E, Klok C, Terblanche J, Chown S (2005) Insect gas exchange patterns: a phylogenetic perspective. J Exp Biol 208:4495–4507
Matthews P, Terblanche J (2015) Evolution of the mechanisms underlying insect respiratory gas exchange. In: Advances in insect physiology, vol 49, pp 2–19. https://doi.org/10.1016/bs.aiip.2015.06.004
Mattingly JC (1999) Ergodicity of 2D Navier–Stokes equations with random forcing and large viscosity. Commun Math Phys 206(2):273–288. https://doi.org/10.1007/s002200050706
Mellanby K (1934) The site of loss of water from insects. Proc R Soc Lond Ser B Biol Sci 116(797):139–149
Monnier N (2013) Bayesian inference approaches for particle trajectory analysis in cell biology. PhD thesis, Harvard University
Montiel D, Cang H, Yang H (2006) Quantitative characterization of changes in dynamical behavior for single-particle tracking studies. J Phys Chem B 110(40):19763–19770
Persson F, Lindén M, Unoson C, Elf J (2013) Extracting intracellular diffusive states and transition rates from single-molecule tracking data. Nat Methods 10(3):265
Rudnicki R, Tyran-Kamińska M (2017) Piecewise deterministic processes in biological models. Springer

Schmalfuß B (1996) A random fixed point theorem based on Lyapunov exponents. Random Comput Dyn 4(4):257–268
Schneiderman H (1960) Discontinuous gas exchange in insects: role of the spiracles. Biol Bull 119:494–528
Schneidermann H (1956) Spiracular control of discontinuous respiration in insects. Nature 170:1169–1171
Slator PJ, Burroughs NJ (2018) A hidden Markov model for detecting confinement in single-particle tracking trajectories. Biophys J 115(9):1741–1754
Slator PJ, Cairo CW, Burroughs NJ (2015) Detection of diffusion heterogeneity in single particle tracking trajectories using a hidden Markov model with measurement noise propagation. PLoS One 10(10):e0140759
Sungkaworn T, Jobin ML, Burnecki K, Weron A, Lohse MJ, Calebiro D (2017) Single-molecule imaging reveals receptor-g protein interactions at cell surface hot spots. Nature 550(7677):543–547
Thorpe WH, Crisp DJ (1947) Studies on plastron respiration. II. The respiratory efficiency of the plastron in aphelocheirus. J Exp Biol 24:270–303
Weis-Fogh T (1964) Diffusion in insect wing muscle, the most active tissue known. J Exp Biol 41(2):229–256
Weron A, Burnecki K, Akin EJ, Solé L, Balcerek M, Tamkun MM, Krapf D (2017) Ergodicity breaking on the neuronal surface emerges from random switching between diffusive states. Sci Rep 7(1):1–10
Wigglesworth V, Gillett J (1936) The loss of water during ecdysis in rhodnius prolixus stRal (hemiptera). In: Proceedings of the royal entomological society of London. Series A, general entomology. Wiley Online Library, vol 11, pp 104–107
Wigglesworth VB (1965) The principles of insect physiology, 6th edn. Methuen
Wigglesworth VB (1931) The respiration of insects. Biol Rev 6(2):181–220. https://doi.org/10.1111/j.1469-185X.1931.tb01026.x
Woods H, Smith J (2010) Universal model for water costs of gas exchange by animals and plants. PNAS 107:8469–8474
Wu Y, Han B, Li Y, Munro E, Odde DJ, Griffin EE (2018) Rapid diffusion-state switching underlies stable cytoplasmic gradients in the *Caenorhabditis elegans* zygote. Proc Natl Acad Sci 115(36):E8440–E8449